2009-01-01

Investigation of the Light Induced Redistribution of BETA Nanoparticles in an Acrylamide-based Photopolymer

Elsa Leite
Dublin Institute of Technology

Izabela Naydenova
Dublin Institute of Technology, izabela.naydenova@dit.ie

Nitesh Pandey
Dublin Institute of Technology

Tzvetanka Babeva
Dublin Institute of Technology

G. Majano
Laboratoire de Matériaux à Porosité Contrôlée, UMR-7016 CNRS

See next page for additional authors

Recommended Citation

Leite, E. et al. (2009) Investigation of the light induced redistribution of zeolite beta nanoparticles in an acrylamide-based photopolymer. *Journal of Optics A: Pure and Applied Optics*, vol. 11, no. 2. doi:10.1088/1464-4258/11/2/024016

Investigation of the light induced redistribution of BETA nanoparticles in an acrylamide-based photopolymer

E. Leite[1*], I. Naydenova[1], N. Pandey[1], T. Babeva[1], G. Majano[2], S. Mintova[2] and V. Toal[1]

[1]*School of Physics, Kevin Street, DIT, Dublin 8, Ireland*

[2]*Laboratoire de Matériaux à Porosité Contrôlée, UMR-7016 CNRS, 68093 Mulhouse, France*

We report redistribution of colloidal zeolite Beta nanoparticles during holographic recording in acrylamide-based photopolymers. Using the techniques of confocal Raman Spectroscopy and Scanning Electron Microscopy coupled with Energy Dispersive X-Ray (SEM-EDX), we have observed a periodic pattern, whose spacing agrees with the fringe spacing of the recorded holographic diffraction grating. It was estimated that the fraction of nanoparticles redistributed as a result of the holographic recording is 40%.

The effect of the nanoparticles on the average refractive index of the nanocomposite layers was studied by UV-visible spectroscopy. It was observed that the addition of zeolite nanoparticles leads to an increase of the photopolymer layers thickness and this is ascribed to the interaction between molecules of monomer and the zeolite nanoparticles, further supported by Raman spectroscopic studies, indicating that these nanoparticles are not an entirely inert additive. The holographic recording properties of the new nanocomposite were characterised and no significant improvement of the net refractive index modulation is observed. This result is explained after taking into account two main factors influencing the final refractive index

modulation – the redistribution of the nanoparticles and the change in the monomers volume concentration due to change in the thickness of the solid layers. The results presented here contribute to insights about the role of nanoparticles in the mechanism of holographic recording in acrylamide based photopolymeric systems. The achieved zeolite nanoparticles redistribution in this new nanocomposite could be useful for fabrication of holographic sensors, as demonstrated by initial studies with toluene.

OCIS codes: 090.2900, 090.7330, 160.2900, 160.5335

1. INTRODUCTION

In recent years, photopolymers have attracted much attention since they have many advantages as holographic materials, such as self-development, wide spectral sensitivity and relatively low cost [1,2]. Extensive research on photopolymers for holographic applications has been reported with significant activity in holographic memories design [3-9], holographic sensors and [10-12] holographic optical elements [13].

Ideally, photopolymer systems for holographic applications should produce large refractive index modulation, in order to obtain high diffraction efficiency and high data storage density, with high dimensional stability to avoid distortion of the recorded holograms due to volumetric changes or shrinkage upon polymerization [14].

In order to minimize the above problems, Bunning *et al.* [15] introduced the idea of introducing inorganic nanoparticles, having substantially higher (or lower) refractive index, n, in

photopolymer mixtures, as a movable non-reactive component. Later the idea of adding inorganic nanoparticles was further developed by other groups [16-18], particularly Tomita et al. Particularly successful was the application of high refractive index TiO_2 nanoparticles (n=2.55, bulk), but other nanoparticles with different refractive indices have been used, such as ZrO_2 (n=2.1, bulk), [19] ZrO_2/TiO_2 [14], SiO_2 (n=1.46, bulk) [20-21] and zirconium isopropoxide [22]. In addition to obtaining much larger refractive index modulation when compared with conventional all-organic photopolymers, the inclusion of nanoparticles also resulted in substantial suppression of polymerization shrinkage, giving high dimensional stability [1,23].

Here the organic host acrylamide based photopolymer is doped with microporous molecular sieve (zeolite Beta) nanoparticles. Zeolite beta belongs to the class of crystalline aluminosilicalites, where the 3-Dimensional structure arises from a framework of $[SiO_4]^{4-}$ and $[AlO_4]^{5-}$ coordination polyhedra linked by all their corners. The frameworks are open and contain channels and cavities in which are located cations and water molecules [24]. Zeolite Beta (BEA-type structure) is a large-pore microporous material with two types of openings (about 6.4Å × 7.6 Å and 5.5 Å × 5.5 Å) prepared from colloidal precursor solutions and characterized by three sets of mutually perpendicular channels with 12-membered ring apertures [25, 26]. The Beta zeolite framework type structure can be seen in more detail in figure 1. Zeolites are hydrophilic due to the interaction of the dipole of the H_2O molecule with the electrostatic fields of the anionic aluminosilicalite framework and the balancing non-framework cations [27].

The main features of the Beta structure make the material suitable for numerous applications including heterogeneous catalysis, sensors, membranes and low-k layers [28, 29].

Zeolite Beta films proved to be effective for water vapour sensing purposes. High sensitivity, good reversibility and long life were demonstrated for this type of zeolite film at low water concentrations. The Beta films show high vapour sorption capacity for different hydrocarbons (pentane, hexane and cyclohexane) [30]. The incorporation of zeolites into composite matrices for membrane applications has been particularly successful [31, 32].

It has been proposed [15, 23] that photopolymer components can be spatially redistributed during holographic recording and if nanoparticles with appropriate refractive index are used, this can lead to a significant improvement in the ultimate refractive index modulation. One of the proposed mechanisms of nanoparticle redistribution is that this effect can be explained by mass transport phenomena. Upon spatially nonuniform illumination by an optical interference pattern a photon of light is absorbed by the dye, producing free radicals. These free radicals can react with the monomer molecules in the bright regions, initiating chain polymerization reactions. Due to the decrease of the chemical potential of the monomers in the bright regions, free monomers migrate (diffuse), replacing those which have polymerized. On the other hand, photo-insensitive non-reactive nanoparticles, which are not consumed in the polymerization process, undergo counter-diffusion from the bright to the dark regions, and their chemical potential increases in the bright regions due to consumption of the monomer. This polymerization-driven mutual diffusion process, leading to phase separation continues until the process of photopolymerisation is complete. The combination of non-uniform polymerization and free monomer diffusion results in a compositional and density difference between the bright and the dark regions, creating a spatial modulation of the refractive index. The effect of Si-MFI zeolite nanoparticles on the final refractive index in acrylamide-based photopolymers [1]

suggests that they are expelled from the bright to the dark fringes areas, in the opposite direction to monomer diffusion. Similar observations, by means of Transmission Electron Microscopy (TEM) [33] and Electron-Probe MicroAnalysis (EPMA) have been reported in other photopolymer systems doped with solid nanoparticles [20].

The studies reported so far have been focused mainly in the evaluation of holographic properties such as dynamic range and level of shrinkage, which are relevant parameters in data storage applications. Most of the proposed models so far explain the holographic gratings diffraction efficiency improvement by the fact that the inorganic nanoparticles are inert and take part only in mass transport mechanism during holographic exposure, as described before. But recently, Goldenberg et al. [34] has proposed a new mechanism of the refractive index contrast amplification in new functionalized acrylate monomers and gold nanoparticles in which the non inert inorganic nanoparticles were found to promote the monomer spatial segregation in addition to mass transport effects.

Here we show the first evidence of redistribution of porous nanoparticles (colloidal Beta zeolite in self -processing water soluble acrylamide-based photopolymers subject to patterned illumination, by means of Scanning Electron Microscopy coupled with Energy Dispersive X-Ray Fluorescence and Raman Spectroscopy. Unlike in Si-MFI doped photopolymer [1] the dynamic range obtained with the inclusion of the BEA nanoparticles in the acrylamide based photopolymer has not increased due to the redistribution effect observed. Raman studies of the photopolymerisable nanocomposite reveals that the monomer molecules associate with the zeolite nanoparticles. Also a double increase of the thickness for a load of beta nanoparticles of

5%wt occurs, indicating the presence of a physical/ chemical interaction between the photopolymer components and the nanoparticles. Such increase in the solid layers thickness when they are produced from the same amounts of stock solutions containing the same amount of each photopolymer component (except for the zeolite nanoparticles) in the doped layers results in variation of the monomers volume concentrations. This could partially or completely cancel the effect of mass transport and the expected refractive index modulation change due to difference of the density in the bright and the dark regions. The novelty of using this nanoparticles arises from the combination of their molecular sieves properties and the fact that a patterned material can be created by means of holographic exposure. Preliminary experiments conducted with toluene, confirmed that the new nanocomposite is promising for the fabrication of holographic sensing applications.

2. MATERIALS AND METHODS

2.1 Materials

The holographic recording material consists of a solution of acrylamide-based photopolymer prepared as described previously [35] doped with several different concentrations of zeolite Beta nanoparticles [25].

Briefly, the acrylamide based photopolymer consists of 2 ml of triethanolamine was added to 9 ml of a polyvinyl alcohol (PVA) solution (20 %wt.). The monomers i.e. 0.6 g of acrylamide and 0.2 g of N,N'-methylenebisacrylamide were then added. The solution was stirred

for 20 minutes and then 4 ml of erythrosine B solution (0.11 %wt.) were added finally and stirred for a further 10 minutes.

The Beta zeolite nanoparticles are prepared from clear precursor solutions containing an excess of organic template. The chemical composition is: 9TEAOH: 0.25 Al_2O_3: 25 SiO_2: 295 H_2O. Aluminum isopropoxide (Acros Organics), silica solution [Ludox SM 30%] (Aldrich), tetraethylammonium hydroxide [TEAOH 20 %wt.] (Aldrich) and distilled water were used as starting materials. The precursor solution was mixed under vigorous stirring for 24h until clear. This solution was further subjected to crystallization in polypropylene bottles at 100^{o}C for 3 days. The crystalline nanoparticles were extracted from the parent liquid by two-step centrifugation (20,000 rpm for 1h) and redispersed in doubly distilled water in an ultrasonic bath for 1h. The stabilized zeolite nanoparticles in water suspension had a pH of 8 and a solid concentration of 1.3 %wt. Dynamic light scattering (DLS) measurements were carried out to determine the mean hydrodynamic diameter of the crystalline zeolite particles, and it was found to be about 40 nm.

Before use, the nanoparticle solution was ultrasonicated for 30 minutes to disperse the nanoparticles homogeneously. The nanoparticle solution was then added to the photopolymer solution and the mixture again ultrasonicated for further 30 minutes In order to obtain a dry photopolymer layer a volume of 0.5 ml of nanocomposite solution was deposited on 38x26cm^2 glass substrate and dried for 24 hours.

2.2. Methods

Holographic recording: the nanocomposite layers were exposed to two mutually interfering s-polarized beams of wavelength 532 nm. The intensity ratio of the two recording beams was kept the same and the exposure intensity was 5 $mWcm^{-2}$. The recording beams were incident on the sample in an unslanted configuration and holographic gratings of several spatial frequencies were recorded, using a total exposure energy of 0.6 Jcm^{-2}. The grating growth was monitored in real time by probing with a beam of He-Ne laser wavelength 632.8 nm incident at the Bragg angle. The sample was held in a rotational stage for adjusting the incident angle of the probe beam to enable the angular selectivity profile to be measured. The maximum diffraction efficiency was calculated using the first diffraction order of the probe beam and together with the effective optical thickness of the grating, determined from the Bragg angular selectivity curve was used in the calculation of refractive index modulation amplitude, Δn, using Kogelnik's coupled wave theory for a volume phase grating [36].

Raman spectroscopy: the Raman spectra from the composite materials were recorded using a Jobin Yvon Raman Spectrometer, equipped with an Ar ion laser of 514.5 nm wavelength. An XYZ motorized stage equipped with a microscope Olympus BX40 was used. The laser was focused on different points in the samples using objective lenses ranging in magnification from 20 to 100x. The Raman spectrometer grating has 1800 $linesmm^{-1}$ resolution.

SEM-EDX: the Scanning Electron Microscopy coupled with Energy Dispersive X-Ray (SEM-EDX) was performed using a Philips XL 30 FEG instrument.

DLS Measurements: the average particle size (Z-ave) was determined by Dynamic Light Scattering measurements (Malvern, Zetasizer Nano Series). The polydispersivity Index (PDI) was used as quality control (PDI). Low PDI values indicate a narrow distribution of particles sizes.

Optical properties: the optical properties (volume refractive indices of the photopolymer nanocomposites) were determined by measuring transmittance, T and reflectances R_f and R_b from front (air) side and back (substrate) side of the layers, respectively using a Perkin-Elmer Lambda 900 UV-VIS-NIR spectrophotometer. The simultaneous determination of refractive index, n, extinction coefficient, k and thickness, d of the layers was performed by minimization of the goal function F consisting of discrepancies between measured ("meas") and calculated ("calc") spectra:

$$F = (T_{calc} - T_{meas})^2 + (R_{fcalc} - R_{fmeas})^2 + (R_{bcalc} - R_{bmeas})^2 \quad (1)$$

F was minimized at each wavelength λ in the spectral range from 400-800 nm by a Nelder-Mead simplex method [37] using a dense grid of initial values of n, k and d. Additionally, n and k were determined from combinations (TR_f) and (TR_b) using Newton-Raphson iterative algorithm [38] and thickness values measured with White Light Interferometric profiler. More details about calculation procedure can be found in [39].

For the sensing experiment, gratings recorded at a spatial frequency of 1000 lmm^{-1} and exposure energy of 250 $mJcm^{-2}$ were used. Layers of around 20 μm of undoped acrylamide based photopolymer and beta nanocomposite were exposed to the same concentration of toluene for the same amount of exposure time and their change in the diffraction efficiency after exposure was studied. The dependence of this change with the initial diffraction efficiency was determined.

3. RESULTS AND DISCUSSION

3.1. Holographic Recording of Volume Gratings

Dynamic Light Scattering (DLS) measurements were performed immediately and again 24 hours after mixing and the results showed that there was no aggregation of the Beta nanoparticles in the photopolymer solution (see figure 2). As can be seen in figure 2a, the average size of beta nanoparticles determined by DLS was found to be around 39 nm. After addition of these beta nanoparticles (10% concentration) to the acrylamide based photopolymer they had an average particle size of around 43nm – figure 2b, a value that did not significantly changed for 24 hours afterwards (44nm – figure 2c).

As shown in figure 3, the diffraction efficiency of the layers significantly increased from 35% for undoped to 69% for those doped with 5wt.% Beta zeolite layers. However, when the change in the thickness of the gratings was taken into account in the calculation of the refractive index modulation no increase of the latter with the increase of nanoparticle concentration was observed. The incorporation of 10 %wt. nanoparticles in the photopolymer results in a decrease in the refractive index modulation of around 25% compared to the undoped acrylamide based photopolymer. It can also be observed that, as the percentage of doping increases, the refractive index modulation decreases.

3.2. Redistribution of Beta Nanoparticles During Holographic Recording

Studies using two different techniques were carried out in order to determine if beta nanoparticles redistribution (mass transport effect) occurs in this type of nanocomposite leading to a patterned photopolymer layer.

Scanning Electron Microscopy coupled with Energy Dispersive X-Ray (SEM-EDX) was used to study the redistribution of nanoparticles in the layers as a result of the holographic recording process. SEM pictures of the photopolymer films showing the distribution of silicon and oxygen belonging to the zeolite Beta nanoparticles are shown in Figure 4. The EDX analysis shows that the distribution of the nanoparticles changes from a random pattern on the outside of the grating (Fig. 4, a) to a regular pattern of high and low intensities inside, corresponding to different concentrations of silicon and oxygen clearly originating from the nanoparticles (Fig 4, b). This occurs with a spacing of about 2 μm, which is in good agreement with the spatial frequency of the holographic grating (2 μm spacing between fringes). This indicates that there is a redistribution of the Beta nanoparticles in the surface of the photopolymer of the same spatial frequency as that used during recording.

Additional studies were done using Raman spectroscopy. The results are presented in figures 5 and 6.

Raman spectra of the acrylamide based photopolymer doped with Beta nanoparticles show two well isolated peaks which are absent in the undoped polymer (Fig. 5, b), one at 415 cm^{-1} and other at 673 cm^{-1} originating from C-C-N vibrations of the organic template used for the synthesis of zeolite Beta nanoparticles [25]. We then monitored the variation of the Raman peak intensity at 673cm^{-1} in the direction of the grating vector as this peak was found to be more sensitive to the changes in zeolite concentration.

As can be seen in figure 6, the variation of the Raman peak at 673cm^{-1} intensity in the grating vector direction is cyclic in conformity with the fringe spacing of 5 μm in the grating studied, indicating that there is indeed a redistribution of nanoparticles when a grating is recorded. The spatial frequency of the grating under study was limited by the lateral resolution of the spectrometer which depends on the laser spot diameter (around 1μm) and the motion controller stage. If one assumes that the intensity of the Raman peak at 673cm^{-1} is proportional to the concentration of the Beta zeolite nanodopants one can estimate that around 40% of the nanoparticles are redistributed; this was calculated from the differences between the minimum and maximum Raman intensities observed at the peak at 673cm^{-1}. As expected, the periodical spatial modulation of the Raman signal was not observed in the nanocomposite outside the grating.

3.3. Effect of Properties of Beta Nanoparticles in Holographic Recording

As seen in figure 3, the diffraction efficiency increases as the concentration of the zeolite increases. The reason for this can be explained by the increasing thickness of the doped nanocomposite. The layer of undoped photopolymer has half of the thickness of a 5 %wt. nanocomposite, so we can expect that the monomer fraction per volume unit of material to be double in undoped layers. When we calculate the refractive index modulation this parameter is per unit volume of material. Thus, the direct comparison of the refractive index modulation in beta nanoparticles doped and undoped photopolymer layers can be misleading. In order to avoid that we have implemented the following procedure. First we have compared the refractive index modulation of undoped acrylamide based photopolymer layer possessing the same thickness but half of the quantity of monomer per unit volume with the refractive index modulation in the layer

containing the standard monomers volume concentration ($19gL^{-1}$) and found out that that the ratio between the two is 1.7 in favour of the standard layer. Then we have compared this ratio with the refractive index modulation ratio between Beta zeolite 5 %wt. nanocomposite and the undoped layers which is 1.2. This measured value of 1.2 represents a smaller drop in the refractive index modulation due to the changed layers thickness and consequently in the monomer volume concentration than the expected one of 1.7, showing that the Beta nanoparticles could be effectively contributing to an refractive index contrast amplification, but this effect being masked by the thickness increase effect of non inert beta nanoparticles. Alternatively this observation could be explained in the following manner. If one takes into account the measured refractive index modulation in undoped layer characterised by the same monomer volume concentration as the one in the doped layer of 5 %wt., one can calculate that the expected diffraction efficiency of a grating recorded in 29 μm undoped layer would be 41%. Considering that in the doped layer the observed diffraction efficiency is 69% we can conclude that the increase of diffraction efficiency is not only due to the increased thickness for doped layer but it is also influenced by the redistribution of particles.

The optical properties of acrylamide based photopolymer were measured inside a grating recorded at a spatial frequency of 1000 lmm^{-1} and an exposure of energy of 0.6 Jcm^{-2}). The refractive index changes showed that the volume refractive index for the undoped photopolymeric system was 1.506±0.007. When doped with beta nanoparticles, the photopolymeric nanocomposite presented a dependence of value of refractive index with percentage of doping (for 2.5 %wt. it was 1.497±0.005, for 5 %wt. doping it was 1.452±0.007 and for 10 %wt. doping it was 1.448±0.007). Comparing these values, one can conclude that the

introduction of beta nanoparticles leads to a decrease in the average refractive index of the system.

In order to further clarify the role of the nanoparticles in this nanocomposite the interaction of the monomer and beta nanoparticles was carried out using Raman spectroscopy. This choice was based on the fact that zeolite beta has pores sizes of around 6Å [25]. Hence, besides water molecules, the only component of the acrylamide based photopolymer that can enter inside the pore channel structure of this zeolite is the monomer acrylamide (molecule size of around 5 x 4 Å) [40].

Initially only acrylamide was studied. It was dissolved in water and the solvent was allowed to evaporate. A series of 30 Raman spectra were then taken. It was found that the acrylamide molecules could be in associated (e.g. hydrogen bonding) or free states [41] (Figure 7A 1) and 7A 2), respectively. The associated state can be distinguished from the free state by the appearance of a new peak at lower frequency, as denoted by the black arrow in the figure.

The second study involved a mixture of acrylamide and beta nanoparticles. The two components were mixed in water and then the solvent was allowed to evaporate. A set of thirty Raman spectra was then taken. Analysis of these spectra showed that, in the presence of beta nanoparticles, the acrylamide molecules were now in an associated state (figure 7B).The presence of a shoulder (new peak) at lower frequencies indicates the presence of acrylamide molecules in an associated state (e.g. hydrogen bonding). From these results, one can conclude that there is an interaction between the monomer and the Beta nanozeolites. More detailed

studies of the interaction of acrylamide molecules and beta nanoparticles are also being performed. Raman studies are being confirmed by nuclear magnetic resonance (NMR) spectroscopy. The results of these studies will be published elsewhere.

3.4. Beta Nanocomposite as Holographic Sensor Material

Despite the fact that no improvement of the refractive index modulation was observed in this particular nanocomposite, the fact that the nanodopants can be spatially redistributed can be used in fabrication of holographic sensors. Holographic sensors are devices consisting of a hologram that changes its properties (diffraction efficiency or spectral response) when exposed to analyte containing environment. The main advantages of holographic sensors recorded in photopolymers are that they provide visual information, can be readily mass produced and are relatively cheap.

An example of a sensor based on a transmission grating is presented in figure 8. The exposure of the analyte to the recorded transmission hologram should give a change in the diffraction efficiency estimated by:

$$\Delta\eta = \sin\left(\frac{2n_1 d\pi}{\lambda}\right)\frac{\pi}{\cos\theta\lambda}\times\left[d\Delta n_1 + n_1\Delta d - \left(\frac{n_1 d}{\lambda}\right)\Delta\lambda\right] \qquad (2)$$

Where η is the maximum diffraction efficiency, n_1 is the refractive index modulation, d is the thickness of the layer, λ is the wavelength of light, θ is the angle between the two laser beams, Δn_1 is the change in the refractive index modulation, Δd is the change in the thickness of the layer and $\Delta\lambda$ is the change in the wavelength of light.

It was observed that due to exposure to toluene the diffraction efficiency of the holographic grating decreased and there was a linear dependence between the initial diffraction efficiency and the change of the diffraction efficiency. The effect of toluene on doped layers was much more pronounced. Detailed studies and analysis of these observations are in progress.

4. CONCLUSIONS

The evidences for light induced redistribution of Beta zeolites incorporated in acrylamide-based photopolymer are reported. Scanning Electron Microscopy coupled with Energy Dispersive X-Ray (SEM-EDX) and Confocal Raman Spectroscopy were used for direct investigation of the redistribution. The modulation of the volume fraction of zeolites in the bright and dark regions was estimated to be 40 %. Despite the fact that nanoparticles redistribute during holographic recording and the volume refractive indices of photopolymer changes when doped with beta nanoparticles, the refractive index modulation of the nanocomposite decreases with doping. Simultaneously a significant increase of the physical thickness of the layers is observed (for heavily doped layers the thickness increases with factor more than two). The increase in the thickness of the doped layers leads to decrease in the monomer volume concentration and this compensates the positive effect of the nanoparticles redistribution on the ultimate refractive index modulation finally resulting in lower refractive index modulation of doped layers compared to undoped. The possible interaction between monomer molecules and Beta zeolites confirmed by complementary Raman investigations could be the reason of the observed increase in the doped layer thicknesses.

The fact that during holographic recording a redistribution of the beta zeolites takes place opens new possibilities in the fabrication of holographic sensors. The preliminary studies conducted with toluene show promising results.

This work was supported by the Technological Sector Research: Strand I - Post-Graduate R&D Skills Programme for the provided scholarship. This publication originated from research conducted with the financial support of Science Foundation Ireland (N 065/RFP/PHY085).

REFERENCES

[1] I. Naydenova, H. Sherif, S. Mintova, S. Martin and V. Toal, Proc. SPIE **6252**, 625206.1-625206 (2006).

[2] K. Tsuchida, M. Ohkawa and S. Sekine, Opt. Eng. **46**, 015801 (2007).

[3] D. Waldman, R. Ingwall, P. Dhal, M. Horner, E. Kolb, H.-Y. Li, R. Minns and H. Schild, Proc. SPIE **2689**, 127-141 (1996).

[4] L. Dhar, A. Hale, H. Katz, M. Schilling, M. Schnoes, and F. Schilling, Opt. Lett. **24**, 487-489 (1999).

[5] W. Gambogi, A. Weber and T. Trout, Proc. SPIE **2043**, 2-13 (1993).

[6] S. Gallego, C. Neipp, M. Ortuño, E. Fernández, A. Beléndez and I. Pascual, Op. Commun. **274**, 43-49 (2007).

[7] F. Ling, B. Tong, S. Jiang, B. Wang, and Y. Zhang, J. Opt. Soc. Am. A **24**, 1945-1949 (2007).

[8] L. Carretero, A. Murciano, S. Blaya, M. Ulibarrena and A. Fimia, Opt. Exp. **12**, 1780-1787 (2004).

[9] J. Sheridan and J. Lawrence, J. Opt. Soc. Am. A **17**, 1108-1114 (2000).

[10] I. Naydenova, R. Jallapuram, V. Toal and S. Martin, Appl. Phys. Lett. **92**, 031109.1-031109.3 (2008).

[11] S. Kabilan, A. Marshall, J. Blyth, A. Hussain, Y. Xiaoping, L. Mei-Ching and C. Lowe, Proc. of IEEE Conference on Sensors, 1003-1006 (2004).

[12] A. Marshall, J. Blyth, C. Davidson and C. Lowe, Anal. Chem. **75**, 4423-4431 (2003).

[13] E. Mihaylova, I. Naydenova, B. Duignan, S. Martin and V. Toal, Opt. and Lasers in Eng. **44** 965-974 (2006).

[14] O. Sakhno, L. Goldenberg, J. Stumpe and T. Smirnova, Nanotechnology **18,** 105704 (2007).

[15] R. Vaia, C. Dennis, L. Natarajan, V. Tondiglia, D. Tomlin and T. Bunning, Adv. Mat. **13,** 1570-1574 (2001)

[16] N. Suzuki, Y. Tomita and T. Kojima, App. Phys. Lett. **81**, 4121-4123 (2002).

[17] C. Sanchez, M. Escuti, C. van Heesch, C. Bastiaansen, D. Broer, J. Loos and R. Nussbaumer, Adv. Func. Mat. **15** , 1623-1629 (2005).

[18] W. Kim, Y.-C. Jeong, J.-K. Park, Op. Express **14,** 8967-8973 (2006).

[19] N. Suzuki, Y. Tomita, K. Ohmori, M. Hidaka and K. Chikama, Opt. Express **14**, 12712-12719 (2006).

[20] Y. Tomita, K. Chikama, Y. Nohara, N. Suzuki, K. Furushima and Y. Endoh, Opt. Lett. **31**, 1402-1404 (2006).

[21] N. Suzuki and Y. Tomita, App. Opt. **43**, 2125-2129 (2004).

[22] F. del Monte, O. Martinez, J. Rodrigo, M. Calvo, P. Cheben, Adv. Mater.18, 2014 (2006)

[23] Y. Tomita, SPIE Newsroom, Micro/Nano Lithography & Fabrication (2007).

[24] A. Dyer, *An introduction to zeolite molecular sieves* (John Wiley and sons, 1988).

[25] B. Mihailovab, V. Valtchev, S. Mintova, A.–C. Faust, N. Petkov and T. Bein, Phys. Chem. Chem. Phys. **7**, 2756-2763 (2005).

[26] S. Mintova, M. Reinelt, T. Metzger, J. Senker and T. Bein, Chem. Commun. **3,** 326-327 (2003).

[27] K. Byrappa and M. Haber, Handbook of hydrothermal technology (Noyes publications, 2001).

[28] Z. Wang, A. Mitra, H. Wang, L. Huang and Y. Yan, Adv. Mater. **13,**1463-1466 (2001).

[29] S. Mintova and T. Bein, Adv. Mater. **13**, 1880-1883 (2001).

[30] S. Mintova and T. Bein, Microporous Mesoporous Mat. **50,** 159-166 (2001).

[31] M. Berry, B. Libby, K. Rose, K-H Haas and R. Thompson, Microporous Mesoporous Mat. **39**, 205-217 (2000).

[32] J. Kim and Y. Lee, J. Membrane Sc. **193**, 209-225 (2001).

[33] Y. Tomita, N. Suzuki and K. Chikama, Opt. Lett. **30**, 839-841 (2005).

[34] L. Goldenberg, O. Sakhno, T. Smirnova, P.Helliwell, V. Chechik and J. Stumpe, Chem. Mater. **20**, 4619–4627 (2008).

[35] S. Martin, P. Leclere, Y. Renotte, V. Toal and Y. Lion, Opt. Eng. **33**, 3942-3945 (1994).

[36] H. Kogelnik, Bell. Syst. Tech. J. **48**, 2909 (1969)

[37] W. Press, S. Teukolsky S and W. Veterling, Numerical recipes in C, , Chap. 10, pp 408-410, Cambridge University Press (1992),

[38] F. Abeles and M. Theye, Surf. Sci. **5**, 325-331 (1966).

[39] T. Babeva, R. Todorov, S. Mintova, T. Yovcheva, I. Naydenova and V. Toal, accepted for publication in J. Opt. A: Pure and Applied Opt.

[40] A. Duarte, A. Costa , A. Amado, J mol. Struct., vol. 723, n^{o}1-3, pp. 63-68 (2005)

[41] G. Socrates, Infrared and Raman characteristic group frequencies – Tables and Charts, 3rd ed., Wiley (2001)

Figure captions:

Figure 1. Periodic building unit of the Beta-type zeolite family: view along (a) [001], (b) [010] and (c) [100] of the basic layer; d) the pore structure of zeolite beta

Figure 2. Dynamic Light Scattering size distribution curves (number weighted) of a) Zeolite type Beta [Z-Ave:38.62nm and PDI:0.121]; b) Acrylamide based photopolymer doped with 10 %wt. of beta nanoparticles [Z-Ave:43.36nm and PDI:0.174]; c) Acrylamide based photopolymer doped with 10 %wt. of beta nanoparticles (24 hours later) [Z-Ave:43.74nm and PDI:0.121].

Figure 3. Refractive index modulation (A), Diffraction efficiency (B) and sample's thickness after holographic exposure (C) of acrylamide based photopolymer (0% doping) and acrylamide based photopolymer doped with 1 %, 2.5 %, 5 % and 10 %wt. beta nanoparticles (spatial frequency 1000 lmm^{-1} and recording energy of 0.6 $mJcm^{-2}$)

Figure 4. SEM-EDX images of acrylamide based photopolymer film doped with 5 %wt. of zeolite Beta: A) outside the grating, and B) inside the grating (500 lmm^{-1}, 2 μm grating spacing).

Figure 5. Raman spectra of A) NC - acrylamide-based photopolymer doped with 10 %wt. Beta nanoparticles, B) ABP - acrylamide-based photopolymer, and C) pure zeolite Beta. (200 lmm^{-1}, 5 μm grating spacing). Inset depicts the C-C-N vibrations from the organic template in the zeolite Beta nanoparticles.

Figure 6. Raman spectra scan (grating vector direction, 1 μm steps) of nanocomposite sample A) Outside the grating (spatial frequency of 200lmm^{-1}); B) Inside the grating; C) (dashed line) Sin function; Dots - experimental data), corresponding to a nanoparticle redistribution of 40 % (200 lmm^{-1}, 5 μm grating spacing).

Figure 7. Raman spectra in the region of N-H stretching A) Free acrylamide (1) and associated acrylamide (2) B) Some associated acrylamide in presence of beta nanoparticles (1) and associated acrylamide in presence of Beta nanoparticles (2); Black arrows denote bands due to associated species

Figure 8. Operating principle of a holographic sensor recorded in a zeolite nanocomposite; A– Recording of the grating in the acrylamide based photopolymer doped with beta nanoparticles; B– Exposure of the grating to the selected analyte (in liquid or gas form)

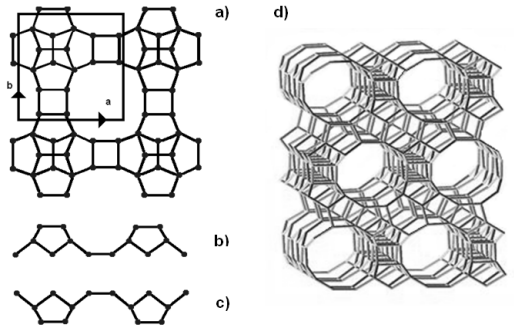

Figure 1. Periodic building unit of the Beta-type zeolite family: view along (a) [001], (b) [010] and (c) [100] of the basic layer; d) the pore structure of zeolite beta

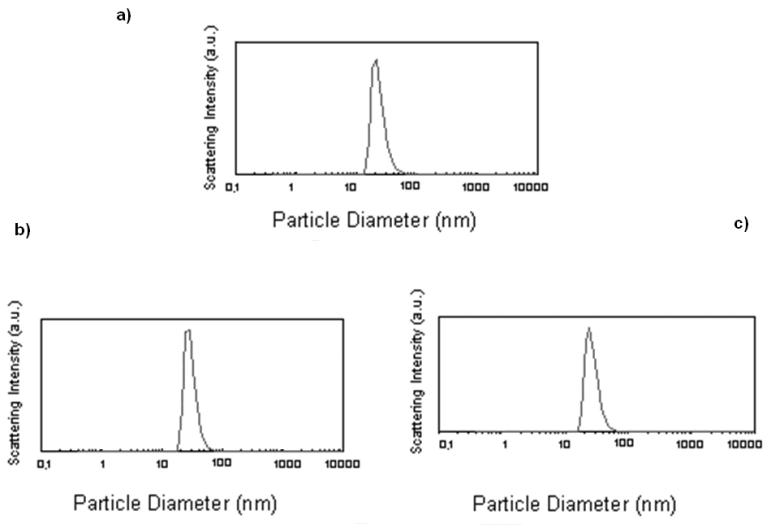

Figure 2. Dynamic Light Scattering size distribution curves (number weighted) of a) Zeolite type Beta [Z-Ave:38.62nm and PDI:0.121]; b) Acrylamide based photopolymer doped with 10 %wt. of beta nanoparticles [Z-Ave:43.36nm and PDI:0.174]; c) Acrylamide based photopolymer doped with 10%wt. of beta nanoparticles (24 hours later) [Z-Ave:43.74nm and PDI:0.121].

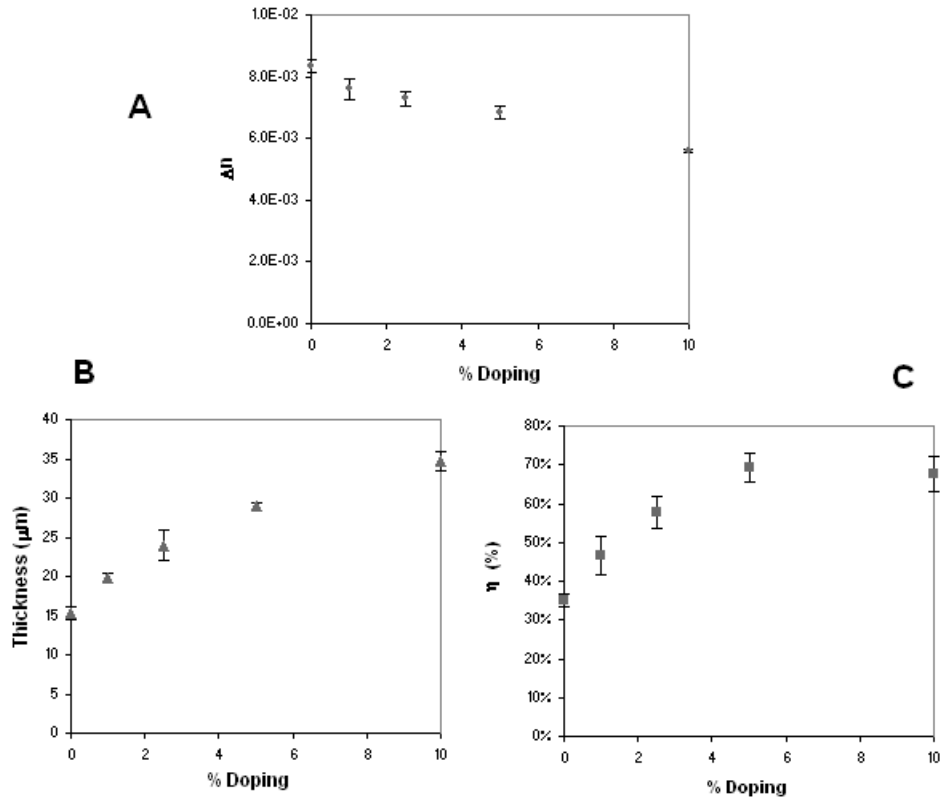

Figure 3. Refractive index modulation (A), Diffraction efficiency (B) and sample's thickness after holographic exposure (C) of acrylamide based photopolymer (0% doping) and acrylamide based photopolymer doped with 1 %, 2.5 %, 5 % and 10 %wt. beta nanoparticles (spatial frequency 1000 lmm^{-1} and recording energy of 0.6 mJcm^{-2})

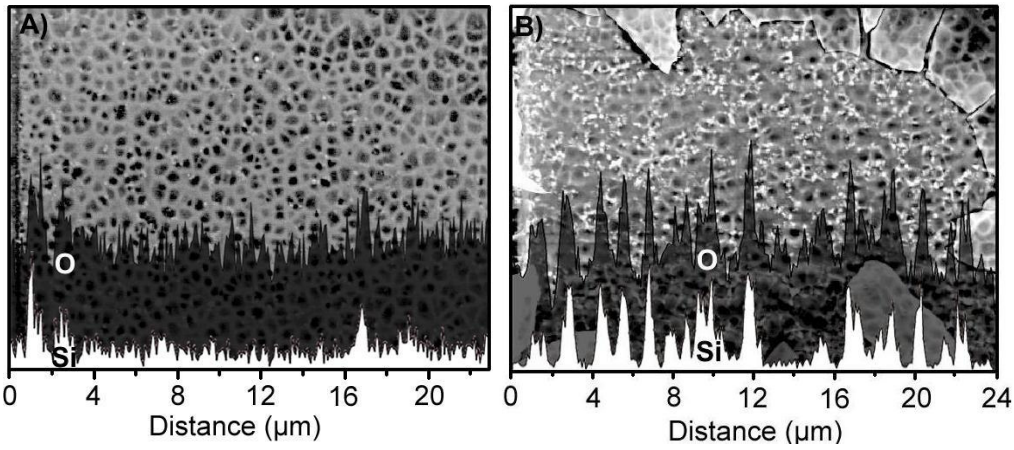

Figure 4. SEM-EDX images of acrylamide based photopolymer film doped with 5 %wt. of zeolite Beta: A) outside the grating, and B) inside the grating (500 lmm^{-1}, 2 μm grating spacing).

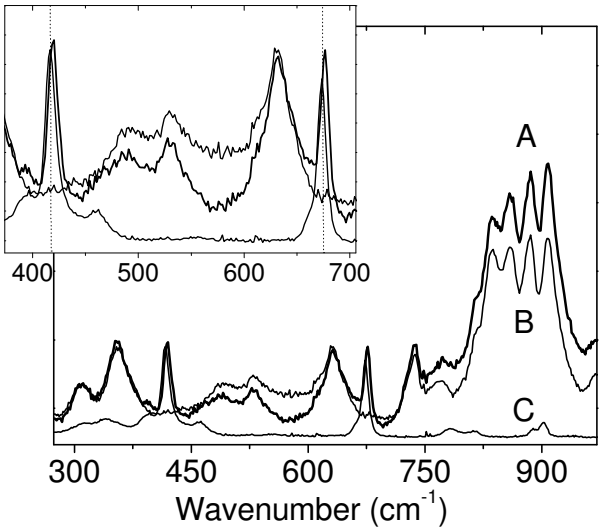

Figure 5. Raman spectra of A) NC - acrylamide-based photopolymer doped with 10 %wt. Beta nanoparticles, B) ABP - acrylamide-based photopolymer, and C) pure zeolite Beta. (200 lmm^{-1}, 5 µm grating spacing). Inset depicts the C-C-N vibrations from the organic template in the zeolite Beta nanoparticles.

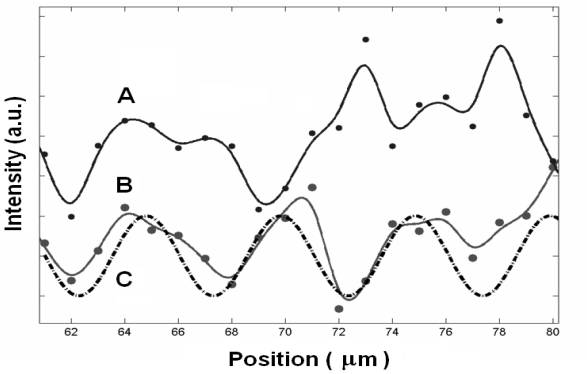

Figure 6. Raman spectra scan (grating vector direction, 1 μm steps) of nanocomposite sample A) Outside the grating; B) Inside the grating; C) (dashed line) Sin function; Dots - experimental data), corresponding to a nanoparticle redistribution of 40 % (200 lmm^{-1}, 5 μm grating spacing).

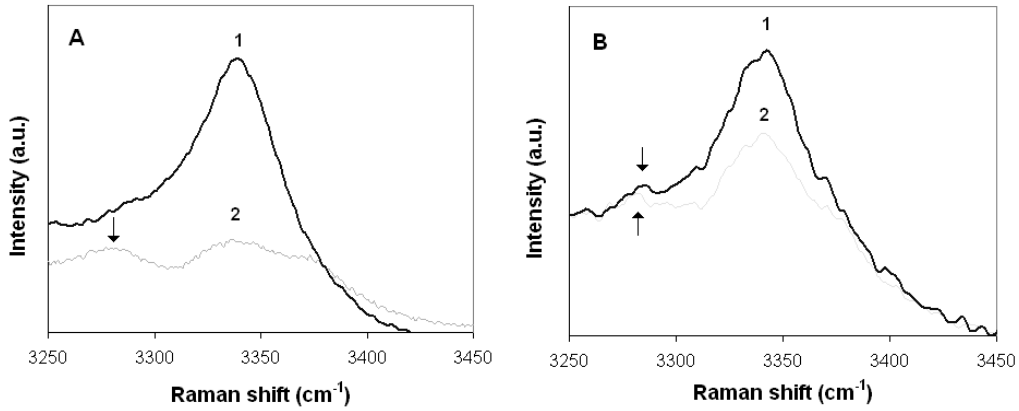

Figure 7. Raman spectra in the region of N-H stretching A) Free acrylamide (1) and associated acrylamide (2) B) Some associated acrylamide in presence of Beta nanoparticles (1) and associated acrylamide in presence of beta nanoparticles (2); Black arrows denote bands due to associated species

Figure 8. Operating principle of a holographic sensor recorded in a zeolite nanocomposite; A – Recording of the grating in the acrylamide based photopolymer doped with beta nanoparticles; B – Exposure of the grating to the selected analyte (in liquid or gas form)